Struct Bond (2012) 149: 159–186
DOI: 10.1007/978-3-642-32753-7_5

Application of Reactivity Indices Within Density Functional Theory to Rationale Chemical Interactions

Abhijit Chatterjee

Abstract Chemistry is the science based on that all process involving bond making and bond breaking. Chemical interactions will determine the activity of the interacting species. If this reaction process can be mimicked by a handy and simple theory to test the validity this can be revolutionary. Reactivity index is that theory which was developed at the right time to rationalize chemical bonding. Density functional theory (DFT) has given precision to chemical concepts such as electronegativity, hardness, and softness and has embedded them in a perturbation approach to chemical reactivity. Since the majority of the reactions can be analyzed through the electrophilicity/nucleophilicity of various species involved, a proper understanding of these properties becomes essential. The hard soft acid–base (HSAB) principles classify the interaction between acids and bases in terms of global softness. In last few years the reactivity index methodology is well established and had found its application in a wide variety of systems. This study is to revisit the definition of reactivity index using DFT, within the domain of HSAB principle and then to discuss its application to rationale chemical interactions; in combination with intra- and intermolecular reactivity in materials.

Keywords Chemical bonding · Chemical interactions · DFT · Material · Reactivity index

Contents

A. Chatterjee (✉)
Accelrys K. K., Kasumigaseki Tokyu Bldg, 17F, 3-7-1 Kasumigaseki, Chiyoda-ku, Tokyo, Japan
e-mail: abhijit.chatterjee@accelrys.com

1 Introduction

Chemistry is the science based on that all process involving bond making and bond breaking. Chemical interactions will determine the activity of the interacting species. This had been long recognized that acids and bases theory remains the most important theory within the space of chemical bond and bonding. The history begins with the pioneering works of Lémery and Boyle in the early 1800 which introduced the "Solubility theory" and the associate principle of reactivity. Next, the major contribution of Rouelle came up, which prescribed the base concept as the complement of that of an acid, with his pneumatic theory of reactions, being culminated by the Lavoisier's contribution according to which the oxygen is directly related to the acidic character of matter. In 1900 Volta, Gay-Lussac and Liebig have preformed the historic physico-chemical experiments in elucidating the fact that acids have to contain hydrogen to be exchanged with a metal and a "radical" of different nature; they established the famous principle:

$$\text{acid} + \text{base} \leftrightarrow \text{salt} + \text{water}. \tag{1}$$

The first overall concept of acid–base was formulated by the Arrhenius, Van't Hoff, and Ostwald in the 1880s, leading to a picture where acids and bases release hydrogen and hydroxide ions, respectively, their interaction being responsible for the acid–base reactions. In the twentieth century, the acid and base definitions get a leap of the century when it happened to link with newly emerging quantum theory of atoms and molecules. The first theory belongs to Brønsted and Lowry [1] (1923), which assumes the proton as the particle, never free, which intermediates between an acid (the donor) and a base (the acceptor) compounds during chemical reactions. Within this framework the new acid–base interaction paradigm looks like:

$$\text{acid1} + \text{base2} \leftrightarrow \text{acid2} + \text{base1}. \tag{2}$$

Although efficient, this theory excessively enhanced the role of proton; fortunately, Lewis' intuition (1916) [2], the electron pair was soon recognized as a more

general conceptual tool in defining acids, bases, and their chemical bonding removing the unnecessary emphasis on protons. Worth noting, the Lewis base definition seems to superimpose on the Brønsted–Lowry theory while the acidic Lewis definition covers more general cases. The acid–base theory was refined again on the ground of the molecular orbital theory, derived by Pearson [3–8].

In this context, the chemical bonding and reactions were described in two steps: one step regards the Coulomb interaction, being quantified by the electronegativity index χ, seen as the negative of the chemical potential of the interacting systems [9], and by the associated equalization principle [10]; in the second step, the stability of the newly formed chemical bond is regulated by the so-called chemical hardness index η, seen as the second-order effect, consequently defined as the chemical force (i.e., the gradient of the chemical potential) acting on the bonding species [11–13]. In molecular orbital terms, the middle point of the HOMO–LUMO gap is associated with the chemical potential (i.e., minus electronegativity), while the weight of the gap is taken as the double of the chemical hardness of that molecule. With these, the acids and bases are further classified as soft ("*s*") and hard ("*h*"): a soft species has electrons easy to be transferred in the vacant orbital (LUMO) whereas the chemical reactions are more favorable as the HOMO level of one species vertically approaches the LUMO of the other. From now on, the molecular systems are recognized as hard and soft acids and bases (HSAB), in the sense that each molecule can be seen as hard–hard, soft–soft, hard–soft or soft–hard bonding combinations between acids and bases. The associate HSAB principle of chemical reactivity was formulated as well, providing that "hard acids prefer hard bases and soft acids prefer soft bases" [14, 15]:

$$h1 - s1 + s2 - h2 \leftrightarrow h1 - h2 + s2 - s1. \tag{3}$$

Despite the qualitative character [16–25] of the HSAB principle, an appropriate quantum index to smoothly distinguish between the soft and hard character of acids, bases, and their bonding, would switch HSAB toward a quantitative theory. A unified picture of the hard-and-soft-acids-and-bases and maximum hardness principles was approached through introducing the maximum hardness index Π. It provides particular chemical hardness ranges where the chemical bonding behaves like hard–hard, soft–soft, and hard–soft or soft–hard acid–base interaction characters and furnishes the key to analytical classification of acids and bases in an intrinsic structural manner. The reliability of the present recipe and index was tested by the chemical hardness ordering predictability and chemical bond nature characterization on a particular series of molecular Lewis acids and bases within various computational and experimental atomic chemical hardness scales. Although a consistent chemical hardness principles and related indices picture was furnished in all cases, considerable differences were noted with respect to the old-fashioned Pearson classification, which is one of the excellent work done by Putz et al. [26–34].

In the heterolytic cleavage of a bond, the electron pair lies with one of the fragments, which becomes electron-rich, while the other fragment becomes electron-deficient. An electron-rich reagent gets attracted to the center of the

positive charge and forms a bond with an electron-deficient species by donating electrons. The electron-rich species is known as a nucleophile, and the electron-deficient one, as an electrophile [35–38]. Free radicals are generated through a corresponding homolytic process where an equal share of one electron is obtained by each fragment. Even radicals are designated as electrophilic/nucleophilic depending on their tendency to attack the reaction sites of relatively higher/lower electron density. Moreover, nucleophiles (electrophiles) are Lewis bases (acids) as well as reducing (oxidizing) agents since they donate (accept) electrons, implying a connection among electrophile–nucleophile chemistry, acid–base chemistry, and oxidation–reduction chemistry.

The chemical potential, chemical hardness and softness and reactivity indices have been used by a number of workers to assess a priori the reactivity of chemical species from their intrinsic electronic properties. The concept of electrophilicity has been known for several decades, although there has not been a rigorous definition of it until recently, Parr et al. [39] proposed a definition did they inspired by the experimental findings of Maynard et al. [40]. The revolution begins, with this simple index which has the ability to connect the major facets of chemical sciences.

Perhaps, one of the most successful and best-known methods is the frontier orbital theory of Fukui [41, 42]. Developed further by Parr and Yang [43], the method relates the reactivity of a molecule with respect to electrophilic or nucleophilic attack to the charge density arising from the highest occupied molecular orbital (HOMO) or lowest unoccupied molecular orbital (LUMO), respectively. According to the definition of global hardness, it is the second derivative of energy with respect to the number of electrons at constant temperature and external potential, which includes the nuclear field, whereas global softness is the inverse of global hardness. The hard soft acid–base (HSAB) principle [44], which was proposed by Pearson, classifies the interaction between acids and bases in terms of global softness. This HSAB principle can be applied successfully for various systems [6, 12, 17, 43, 45–54]. Furthermore, Pearson also suggested another principle of maximum hardness (PMH) [55]. It states that, for a constant external potential, the system with the maximum global hardness is most stable and also studied extensively to further probe into both inter- and intramolecular interactions [56–64]. Incorporation of HSAB concept into the DFT structure has several consequences, such as the hardness scale generated through the HSAB principle classifies chemical species in accordance with their behavior and in a good agreement with experimental values for a large number of cations, atoms, radicals and molecules [65]. On the other hand, Vela et al. suggested a linear relationship of global softness with dipole polarizability and consistent with empirical evidence [66]. In recent days, DFT has gained widespread interest in quantum chemistry. Some DFT-based local properties, e.g. Fukui functions and local softness as reactivity index have already been used for the reliable predictions in various types of electrophilic and nucleophilic reactive species involving in the chemical reactions [67, 68]. Moreover, the reactivity index scale can expand its domain successfully not only to predict the interaction between heteroatom and zeolite framework [69], but in various other fields [70–75].

This produces reliable results for the chemical properties of molecules and solids. DFT calculations are also fairly computationally inexpensive [75], making this the method of choice for accurate calculations on large molecular and solid-state systems. Finally, DFT programs for periodic systems are now widely available [76], making this the method of choice for modeling chemical reactivity on surfaces or within lattices. Such periodic calculations eliminate the uncertainties introduced by using finite-sized cluster approximations. In applications like the ones cited above, the magnitudes of the Fukui Functions (FFs) are correlated with the reactivity of various sites in a molecule. These FFs can be condensed to atomic-centered indices that can be used to predict which sites are most likely to react with electrophiles or nucleophiles. This can be used to compare the activities of sites within a molecule, or can be used as a measure of how various side groups alter the reactivity of a molecule.

The study of material properties based on the experiment is a difficult task because it is a complicated process. Theoretically, quantum mechanics is too simple to predict them. Hence, the application of reactivity index is an advanced and wise choice. Regarding material designing, prediction of the excited state has been considered a challenging and intricate problem as there is not much focus on chemical reactivity involving excited state [76]. In particular, the investigation of excited state properties are generally computed using time-dependent density functional theory (TD DFT). However, the disadvantages of TD DFT are notorious, which does not allow more accurate *ab initio* approaches than random phase approximation (RPA) and configuration interaction with single substitutions CIS. There is no privileged direction for improvement in DFT except changing the parameterized potential, which is not very promising alternative, considering the past experience with semi-empirical methods [77]. Moreover, the computational costs and the complexity experiences are comparable with RPA and CIS method. Hence, the calculation of excited state remains a challenging problem in DFT without involving perturbation. This provoked us to (1) revisit the fact that ground state DFT can reproduce the singlet excited state and (2) verify the process, until which extent the reactivity results can be reliable to explain the excited state behavior by comparing with experimental results. The reactivity index calculation of the ground state and excited state has been performed on closed systems such as methane, benzene and their chlorine substituted compounds. A comparison was made between the geometry of ground state and the excited state for those moieties through configuration interaction (CI) method with Austin Model 1 (AM1) Hamiltonian over the optimized geometry of DFT at the ground state. Results obtained through these two methodologies suggested that in terms of polarizability and heat of formation, DFT can reproduces the trend of excited state qualitatively. Again, those results can be further validated through UV spectral numbers, generated using CI method. The reactivity index proposition based on ground state was comparable with the excited state calculations and has potential to simulate the available experimental numbers.

With this background in this review we will now talk about the basic theory of the reactivity index including definitions of local and global softness along with relative nucleophilicity and electrophilicity. We will as well cover the role of response function in deriving the excited state reactivity index theory, followed

by specific examples on chemical interactions with emphasis on cases where molecular interactions are detrimental for a chemical process.

2 Theory

In density functional theory, hardness (η) is defined as [13]

$$\eta = \frac{1}{2}\left(\frac{\delta^2 E}{\delta N^2}\right)v(r) = \frac{1}{2}\left(\frac{\delta \mu}{\delta N}\right)v, \tag{4}$$

where E is the total energy, N is the number of electrons of the chemical species and the chemical potential.

The global softness, S, is defined as the inverse of the global hardness (η):

$$S = \frac{1}{2\eta} = \left(\frac{\delta N}{\delta \mu}\right)v. \tag{5}$$

Using the finite difference approximation, S can be approximated as

$$S = \frac{1}{(\mathrm{IE} - \mathrm{EA})}, \tag{6}$$

where IE and EA are the first ionization energy and electron affinity of the molecule, respectively.

The Fukui function $f(r)$ is defined by [14]:

$$f(r) = \left[\frac{\delta \mu}{\delta v}(r)\right]_N = \left[\frac{\delta \rho(r)}{\delta N}\right]_v. \tag{7}$$

The function "f" is thus a local quantity, which has different values at different points in the species, N is the total number of electrons, μ is the chemical potential and v is the potential acting on an electron due to all nuclei present. Since $\rho(r)$ as a function of N has slope discontinuities, Eq. (4) provides the following three reaction indices [14]:

$$f^-(r) = \left[\frac{\delta \rho(r)}{\delta N}\right]v^- \quad \text{(governing electrophilic attack)},$$

$$f^+(r) = \left[\frac{\delta \rho(r)}{\delta N}\right]v^+ \quad \text{(governing nucleophilic attack)},$$

$$f^0(r) = \frac{1}{2}[f^+(r) + f^-(r)] \quad \text{(for radial attack)}.$$

In a finite difference approximation, the condensed Fukui function [14] of an atom, say x, in a molecule with N electrons is defined as:

$$fx^{+} = [q_x(N+1) - q_x(N)] \quad \text{(for nucleophilic attack)}, \tag{8}$$

$$fx^{-} = [q_x(N) - q_x(N-1)] \quad \text{(for electrophilic attack)},$$

$$fx^{0} = \frac{[q_x(N+1) - q_x(N)]}{2} \quad \text{(for radical attack)},$$

where q_x is the electronic population of atom x in a molecule.

The local softness $s(r)$ can be defined as

$$s(r) = \left(\frac{\delta\rho(r)}{\delta\mu}\right)_v. \tag{9}$$

Equation (6) can also be written as

$$s(r) = \left[\frac{\delta\rho(r)}{\delta N}\right] v \left[\frac{\delta N}{\delta\mu}\right]_v = f(r)S. \tag{10}$$

Thus, local softness contains the same information as the Fukui function $f(r)$ plus additional information about the total molecular softness, which is related to the global reactivity with respect to a reaction partner, as stated in HSAB principle. Thus the Fukui function may be therefore is thought of as a normalized local softness. Atomic softness values can easily be calculated by using Eq. (7), namely:

$$s_x{}^{+} = [q_x(N+1) - q_x(N)]S, \tag{11}$$

$$s_x{}^{-} = [q_x(N) - q_x(N-1)]S,$$

$$s_x^0 = \frac{S[q_x(N+1) - q_x(N-1)]}{2}.$$

In a recent work, Fitzgerald et al. [78] have shown that fractional charges as opposed to continuum charges can reduce the error in Fukui Index values up to 5 %. DFT is well-suited for use with noninteger occupations. Fractional occupations of orbital are commonly employed in the use of charge smearing to improve self-consistent field (SCF) convergence [79, 80]. Using fractional occupations, the partial derivatives are approximated as

$$f^{-}(\bar{r}) = \left(\frac{\partial\rho(\bar{r})}{\partial N}\right)_v^{-} \cong \frac{1}{\Delta N}\left(\rho_N + \Delta(\bar{r}) - \rho(\bar{r})\right), \tag{12}$$

$$f^{+}(\bar{r}) = \left(\frac{\partial\rho(\bar{r})}{\partial N}\right)_v^{+} \cong \frac{1}{\Delta N}\left(\rho_N + \Delta(\bar{r}) - \rho(\bar{r})\right). \tag{13}$$

There are some anomalous cases in which a specific atom shows both high electrophilicity and nucleophilicity due to the limitation of various basis set-dependent charge calculation procedures, and hence it is more appropriate to rationalize this concept of relative electrophilicity/nucleophilicity. Relative nucleophilicity is the nucleophilicity of a site relative to its own electrophilicity, and vice versa for relative electrophilicity. The idea of relative nucleophilicity/electrophilicity was first proposed by Roy et al. [81] to predict intramolecular reactivity sequences of carbonyl compounds. We have used a similar ratio for the first time to find the best di-octahedral smectite for nitrogen heterocyclics adsorption in terms of intermolecular interaction [82] and as well for the adsorption property of *para* and *meta* substituted nitrobenzene [83].

As the nuclear charge increases for a same number of electrons, the system become harder and more polarizable. A many particle system is completely characterized by total number of electrons (N) and the chemical potential $v(r)$ while χ and η describe the response of the system when N changes at fixed $v(r)$; the linear density response function $R(r, r')$ depicts the same for the variation of $v(r)$ for constant N [76]:

$$R(r\,r') = \left[\frac{\rho\delta(r)}{\delta v(r')}\right]N. \tag{14}$$

This response function can be expressed as

$$R(r\,r') = \left[\frac{s(r)s(r')}{S}\right] - s(r\,r'), \tag{15}$$

where $s(r, r')$, $s(r)$ and S are the softness kernel, local softness, and global softness. The linear response of the chemical species is measured in terms of static electric dipole polarizability in presence of weak external electric field.

It is important to note that the Fukui function and the related quantities may not provide proper reactivity trends for hard–hard interactions. Hard–hard interactions are charge-controlled since they are ionic in nature, whereas soft–soft interactions are frontier-controlled because of their covalent nature. The charge-based descriptors would be better suited to tackle the hard–hard interactions. During an electrophile–nucleophile interaction process, when two reactants approach each other from a large distance, they feel only the effect of the global electrophilicity of each other and not its local counterpart. Moreover, the numerical values of any condensed-to-atom quantity and the resulting trends should be analyzed with caution as they are empirical in nature owing to their dependence on the density partitioning scheme used.

3 Calculation Methodology

In the present study, all calculations have been carried out with DFT [84, 85] using DMol^3 code of Accelrys. A gradient-corrected functional BLYP [43, 86] and DNP basis set [87] was used throughout the calculation. Basis set superposition error

(BSSE) has also been calculated for the current basis set in nonlocal density approximation (NLDA) and the theories for reactivity index calculations were mentioned elsewhere in details [88]. Single-point calculations of the cation and anion of each molecule at the optimized geometry of the neutral molecules were also performed to evaluate Fukui functions as well as global and local softness. The condensed Fukui function and atomic softness was evaluated using Eqs. (8) and (11), respectively and the gross atomic charges were evaluated by the technique of electrostatic potential (ESP) driven charges. Geometries were optimized using analytic gradients and an efficient algorithm, which used delocalized internal coordinates so that the change of energy and the change of the maximum force was 2×10^{-5} Ha, and 0.004 Ha/Å, respectively. The studied molecule with a fixed symmetry was subjected to the electric field of 0.02 Hartree/Bohr parallel to the planar direction of the molecule. A field of ~1 V/Å has been applied to the molecules to calculate the response function.

Local Fukui Functions and global Softness were computed by finite differences with $\Delta N = 0.01$, 0.1 and 1.0. For each system, the DFT energy was converged to self-consistency. Atomic point charges were computed as described below. The SCF calculation was repeated using charges of $\Delta N = 0.01$, 0.1 and 1.0, and the atomic point charges were again computed, and condensed FFs were evaluated. DMol3, the program employs partition functions to divide space into regions associated with an atomic centre. Atomic charges were computed by integrating the charge density over all grid points while applying an appropriate partition function [78]:

$$q_k^H = Z_k - \sum_i \rho(\hat{r}i) \frac{\rho_k(\hat{r}i)}{\rho_T(\hat{r}i)}, \tag{16}$$

where Z_k is the nuclear charge and ρ is the charge density of the isolated atom k,

$$\rho_T(\breve{r}_i) = \sum_j \rho_j(\breve{r}_i). \tag{17}$$

The sum over i runs over all numerical integration points in the molecule and the sum over j includes all atoms. This yields the Hirschfield atomic charges. We designate this type of atomic charge as q_k^H.

4 Application Examples

The reactivity index theory has been developed for the cause of chemical bonding and hence applied to all branches of chemical activity. There are different forms of describing the reactivity index, where the idea is to find the donor/acceptor capability of an atom present in a molecule interacting with another molecule or the interaction is within itself. This is the main concept, now depending on the interaction that is taking place; one can look into local softness of the atom, which is approaching the other interacting species or the group of atoms together

approaching the active site. It has also been mentioned that if one wishes, one can describe the interaction between atoms for an intermolecular interaction through the concept of an equilibrium using the idea of reactivity index. Hence the concept reactivity index tells you the activity of atom center and its capability to interact with other species in its localized/nonlocalized neighbor. In recent years, various applications of reactivity index theory and its detailed description were studied [89]. According to the literature, two main issues are dealt with chemical reactivity index: (1) the chemical reactivity theory approach and its application for resolving chemical concern of importance within the helm of DFT and (2) application of DFT on resolving structure–property relationship in catalysis, reactions, and small molecules. With that background, this is the time again to show that how this theory can be applicable to address issues in industry and our main concerned industries are chemical, pharmaceutical, drug, semiconductor, and also polymers where people wanted to design molecule or material for a specific inter- or intramolecular interaction. Following are the few examples where chemical reactivity index can efficiently apply to shade light on the chemical interactions and rationalize scientific issues.

4.1 Scaling the Activity of Fluorophore Molecules

Anthracenes bearing aliphatic or aromatic amino substituent, which behave as molecular sensors, have shown their potential to act as photon-induced electron transfer (PET) systems. In this PET, the fluorophore moieties are responsible for electron release during protonation and deprotonation. The principle of HSAB deals with both intra- and intermolecular electron migration. It is possible to calculate the localized properties in terms of Fukui functions in the realm of DFT and thus calculate and establish a numerical matchmaking procedure that will generate an a priori rule for choosing the fluorophore in terms of its activity. We calculated the localized properties for neutral, anionic, and cationic systems to trace the course of the efficiency. A qualitative scale is proposed in terms of the feasibility of intramolecular hydrogen bonding. To investigate the effect of the environment of the nitrogen atom on protonation going from mono- to diprotonated systems the partial density of states has been calculated and compared the activity sequence with reactivity indices. The results show that location of the nitrogen atom in an aromatic ring does not influence the PET, but for aliphatic chains it plays a role. Furthermore, the protonation/deprotonation scenario has been explained. The results show that the reactivity indices can be used as a suitable property for scaling the activity of fluorophore molecules for the PET process [73].

4.2 Adsorption of Ozone-Depleting Chlorofluorocarbons

Adsorption of ozone-depleting chlorofluorocarbons (CFC) over zeolite is of major global environmental concern. To investigate the nature of CFCs including fluoro,

chlorofluoro, and hydrofluoro/chloro carbons (CF_4, CF_3Cl, CF_2Cl_2, $CFCl_3$, CHF_3, $CHCl_3$) adsorption first-principle calculation was performed on faujasite models [88, 89]. Experimentally it is observed that separation of halocarbons is possible using Na–Y, though the cause is unknown. Reactivity index within the realm of HSAB principle was used to monitor the activity of the interacting CFCs using DFT to propose a qualitative order. The importance of both H-bonding and cation–F–Cl interactions in determining the low-energy sorption sites were monitored and rationalized. The host–guest interactions show a distinctive difference between the adsorption phenomenon between H–Y and Na–Y and as well for Cl and F. It is observed that Cl has more favorable interaction with hydrogen of H–Y compared to Na–Y and for F, the situation is reversed. To validate this trend periodic optimization calculations were performed. The interaction energy as obtained matches well with the reactivity index order resulted from cluster calculations. This study is a combination of DFT and periodic calculation to rationalize the electronic phenomenon of the chemical interaction process.

4.3 Designing of Stable Clay Nano-Composite

Resorcinol forms a novel nano-composite in the interlayer of montmorillonite. This resorcinol oligomer is stable inside the clay matrixes even above the boiling point of the monomer. A periodic ab initio calculation was performed with hydrated and nonhydrated montmorillonite before and after intercalation of resorcinol [90]. For the most feasible dimer- and tetramer-shaped oligomer of resorcinol, the intramolecular and intermolecular hydrogen bonding feasibility has been tested using the DFT-BLYP approach and the DNP basis set in the gas phase and in the presence of aqueous solvent. After locating the active site through Fukui functions within the realm of the HSAB principle, the relative nucleophilicity of the active cation sites in their hydrated state has been calculated. A novel quantitative scale in terms of the relative nucleophilicity and electrophilicity of the interacting resorcinol oligomers before and after solvation is proposed. Besides that, a comparison with a hydration situation and also the strength of the hydrogen bridges have been evaluated using mainly the dimer and cyclic tetramer type oligomers of resorcinol. In terms of localized reactivity index, the same atomic center of the resorcinol molecule produces the maximum electrophilicity and nucleophilicity. The electrophilicity is increasing after hydration and favors the interaction with the clay lattice with higher nucleophilicity. The monomers of resorcinol therefore can combine in the presence of water. As the monomers combine to form dimers or higher oligomers, their activity toward interaction with the clay interlayer increases. Localized reactivity calculation thus can propose the path of the interaction and its feasibility.

Using periodic ab-initio calculations, the formation mechanisms were traced: (1) resorcinol molecules combine without any interaction with water or (2) resorcinol oligomerizes through water. Both the mechanisms are compared and the effect of water on the process is elucidated. The results show that resorcinol molecules

combine after hydration only and hence they are stable at higher temperature. The fittings of the oligomers were also tested as well by periodic calculation to compare the stability of the oligomers inside the newly formed clay nanocomposite.

4.4 Effect of Dopants on Bronsted and Lewis Acid Site

The influence of both bivalent and trivalent metal substituent from a range of metal cation (Co, Mn, Mg, Fe, and Cr) on the acidic property (both Brönsted and Lewis) of metal-substituted aluminum phosphate MeAlPOs is monitored [91]. The influence of the environment of the acid site is studied both by localized cluster and periodic calculations to propose that the acidity of AlPOs can be predictable with accuracy so that AlPO material with desired acidity can be designed. A semiquantitative reactivity scale within the domain of HSAB principle is proposed in terms of the metal substitutions using DFT. It is observed that for the bivalent metal cations Lewis acidity linearly increases with ionic size, whereas the Brönsted acidity is solely dependent on the nearest oxygen environment. Intramolecular and intermolecular interactions show that once the active site of the interacting species is identified, the influence of the environment can be prescribed. Mg^{+2}-doped AlPO-34 exhibits highest Brönsted acidity, whereas Cr^{+3}-doped species shows lowest acidity. Fe^{+2}–Fe^{+3}-doped AlPO-34 shows highest Lewis acidity, whereas Mn^{+2}, Mg^{+2} shows lowest acidity.

The cluster calculations were formed on localized cluster generated from the AlPO-34 structure with the terminal Al or P. Two independent clusters of the formula (1) $M^{+2}AlP_2O_{12}H_9$ and (2) $M^{+3}AlP_2O_{12}H_8$ generated by replacing one P by a M^{2+} or M^{3+} to represent the bivalent and trivalent dopant incorporated clusters respectively as shown in Fig. 1. The proton is included at the bridging oxygen where the dopant is incorporated for electrical neutrality for bivalent substitution. The terminal Al or P was replaced by hydrogen at that distance to mimic the real situation. It is observed that for the bivalent dopants the local environment is a distorted tetrahedral. For all the cases the M–OH distance is the longest. The M–O distances are considerably longer than the Al–O distance when the AlPO material is undoped, showing that the dopants introduce a considerable amount of distortion in the system. There is a drastic change in the M–O–P and angle values, ~135^0 compared to the Al–O–P ~148^0, which show that the observed structural distortion is not local and can be propagated beyond the nearest neighbor to the undoped region, which is in sharp contrast to the earlier results of Saadoune et al. [92]. To correlate the activity of dopants, hence we performed localized reactivity index calculation for the bivalent dopants using $M^{+2}AlP_2O_{12}H_9$ cluster. The Fukui function and local softness for the hydroxyl proton is presented both in terms of nucleophilic and electrophilic activity. Relative electrophilicity (s_x^+/s_x^-) and relative nucleophilicity (s_x^-/s_x^+) can be defined as the electrophilicity of any site as compared to its own (nucleophilicity for the first term and vice versa). The results are shown in Table 1. The cluster chosen was shown in Fig. 1.

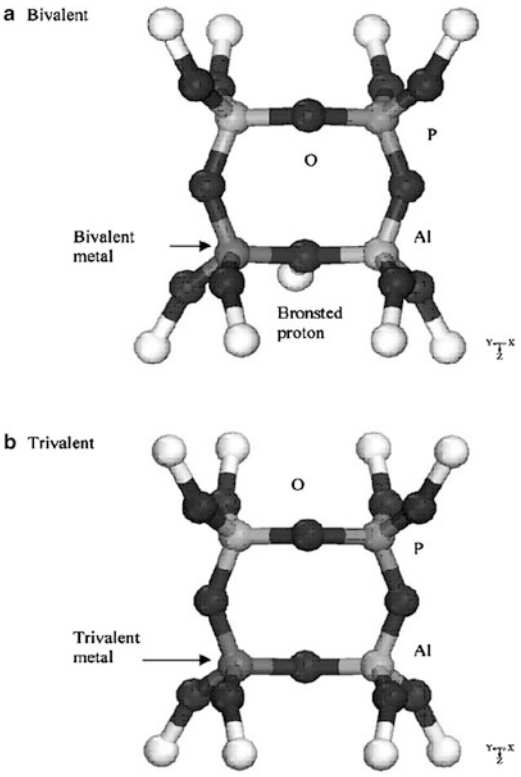

Fig. 1 Two independent cluster with the formula (**a**) $M^{+2}AlP_2O_{12}H_9$ and (**b**) $M^{+3}AlP_2O_{12}H_8$ to represent the bivalent and trivalent dopant incorporated clusters

Table 1 Local softness and relative nucleophilicity for the bivalent dopants calculated in terms of the hydroxyl proton using ESP charges by DFT to monitor Bronsted acidity trend

Metal ion	s_x^+	s_x^-	s_x^+/s_x^-
Mg^{2+}	0.20	0.53	2.555
Mn^{2+}	0.37	0.32	1.156
Cr^{2+}	0.43	0.44	0.977
Co^{2+}	0.53	0.36	1.478
Fe^{2+}	0.53	0.44	1.204

The results show that the relative nucleophilicity is highest for Mg^{2+} and is lowest for Cr^{2+}, which is opposite to the trend observed in terms of substitution energy. Fukui functions were used to monitor the dopant's activity in terms of Lewis acidity. For bivalent cation this order is totally different form the order obtained in terms of substitution energy and that obtained from the Bronsted acidity trend. For the trivalent dopant the highest and the lowest is for Mn^{3+}; the results match with the trend of substitution energy. The trend for Bronsted acidity is $Cr^{2+} < Mn^{2+} < Fe^{2+} < Co^{2+} < Mg^{2+}$, whereas the trend for Lewis acidity mainly for trivalent metal dopant is $Fe^{3+} > Co^{3+} > Cr^{3+} > Mn^{3+}$. This optimistic result

encourages us to monitor a mixed valence situation, which may ideally exist during calcinations for the cations with variable oxidation state.

4.5 Effect of Solvation on the Interaction of Chromophore

Amino-functional silanol surface is mostly used for the immobilization of inorganic ions, molecules, organic, or biochemical molecules onto the mesopore surface. In analytical chemistry, the metal ion uptake was visualized through colorimetric sensors using chromophore molecules. One needs to know the structure–property correlation between the chromophore and silylating agent while choosing chromophore, which is very important to design the sensors. We have used two chromophores representative of hydrophobic and hydrophilic type and used density functional calculation on all the interacting molecules in both the unsolvated phase and solvated medium within the domain of HSAB principle to look at the localized activity of the interacting atoms of these reacting molecules to formulate a rule to choose the best chromophore. The mechanism of interaction between chromophore and the silylating agent has also been postulated. The results were compared with experiment and it is observed that solvation plays a detrimental role in the binding of chromophore with silylating agent. The results also show that the range of reactivity index can be used as a suitable property to scale activity of chromophore molecules suitable for the sensing process. It is observed that the hydrophobic chromophore binds stronger with both the metal and the silylating agent whereas for the hydrophilic one, it binds only with the silylating agent when solvated and in all cases the metal ion binding is weaker compared to that of the hydrophobic one [93].

In terms of global softness the order of activity for the chromophores both when solvated and unsolvated is as follows: PAR $>$ ZINCON. PAR shows much higher global softness than ZINCON, even compared to that of TMAC. In terms of dipole moment ZINCON shows greater hydrophilicity compared to TMAC when unsolvated. But TMAC is more hydrophilic than the ZINCON when solvated. At the same time it shows the greater hydrophobicity for PAR. We will now compare the atomic center of the silylating agent with highest relative electrophilicity/nucleophilicity to match with the counter active atom from chromophore with highest nucleophilicity/electrophilicity for pseudo bond formation. Based on these results one can foresee the interaction between the molecules as shown in Fig. 2 to propose the intramolecular chemical interaction.

4.6 Prediction of Interaction Between Metal Clusters with Oxide Surface

The HSAB principle classifies the interaction between acids and bases in terms of global softness. In last few years, the reactivity index methodology is well

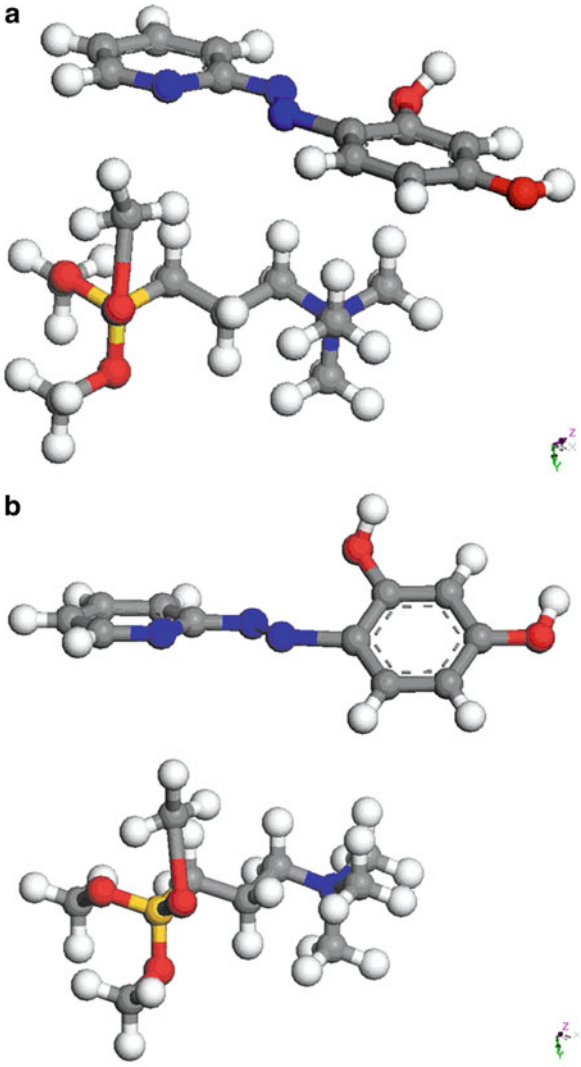

Fig. 2 Interaction between *N*-trimethoxysilylpropyl *N*,*N*,*N*-trimethyl ammonium chloride (TMAC) and 4-(2-pyridylazo)-resorcinol (PAR). (**a**) Unsolvated. (**b**) Solvated

established and had found its application in a wide variety of systems. This study deals with the viability of the reactivity index to monitor metal–cluster interaction with oxide. Pure gold cluster of a size between 2 and 12 was chosen to interact with clean alumina (100) surface. A scale was derived in terms of intra- and intermolecular interactions of gold cluster with alumina surface to rationalize the role of reactivity index in material designing [94].

We have calculated the relative nucleophilicity and electrophilicity for the clusters in the middle of the table, left hand side is for pure clusters and right hand side is for the clusters adsorbed over alumina surface.

Table 2 The relative electrophilicity and nucleophilicity of the individual atom centers in the gold cluster (left) before adsorption and the gold cluster after adsorption over alumina surface (right)

s_x^+/s_x^-	s_x^-/s_x^+	M	s_x^+/s_x^-	s_x^-/s_x^+
9.23	0.30	Au5(Td)	3.79	0.26
7.56	0.67	Au5(C4V)	3.73	0.27
6.91	0.14	Au6	4.43	0.22
5.38	0.18	Au7	4.11	0.24
5.30	0.19	Au8	5.36	0.19
5.76	0.17	Au9	6.86	0.15
5.66	0.15	Au10	8.71	0.11
5.37	0.16	Au11	11.51	0.09
5.17	0.11	Au12	15.00	0.07

From the results of Table 2 it is observed that the relative electrophilicity decreases with increase in the cluster size. That means that intramolecular interaction decreases with increase in cluster size as also justified by localized directive Fukui function numbers from the same table. The relative nucleophilicity really produces a very opposite trend with alumina clusters. The activity is increasing with the size now, which is just opposite to the trend for the pure gold cluster activity. This proposes that the clusters with bigger size will remain active after adsorbing over alumina surface.

4.7 Study on CDK2 Inhibitors Using Global Softness

The reactivity index is as well popular in pharmaceutical and drug applications. In particular, one problem of drug design is that one has to synthesize and screen thousands, sometimes millions, of candidate chemicals in developing one successful drug. There was a very successful study with reactivity index long back on human immunodeficiency virus (HIV) [95]. The cyclin-dependent kinases (CDKs) are a class of enzymes involved in the eukaryotic cell-cycle regulation.

A recent theoretical study on a series of CDK2 inhibitors used a set of global reactivity indices defined in terms of the density of states [96]. The related series were classified on the basis of the correlations obtained for the complete set of compounds and the sites targeted within the active site of CDK2. The comparison between the biological activity and the electronic chemical potential obtained through Fermi level yields poor results, thereby suggesting that the interaction between the hinge region of CDK2 and the ligands may have a marginal contribution from the charge transfer component. The comparison between the biological activity and global softness shows a better correlation, suggesting that polarization effects dominate over the CT contribution in the interaction between the so-called hinge region and the ligand. This result is very encouraging to show that the role of reactivity index in the intermolecular interaction, which can be further extrapolated to the intermolecular region to study the occupied states.

4.8 Molecular Interaction in Polymerization Reaction

Indeed, despite its many good characteristics, such as its long lifetime and the fact that this material is easy to process, the low thermal stability of PVC caused by the occurrence of side reactions in the polymerization process remains a problem. These side reactions lead to structural defects within the polymer, which have a great impact on the characteristics of the product. Better insight into the mechanism of these side reactions and their degree of reversibility would be helpful for improving the industrial production processes or, for PVC in particular, to reduce, for instance, the addition of environment-affecting thermal stabilizers during processing. A detailed investigation of the kinetic irreversibility–reversibility concept is presented on the basis of the analysis of four side reactions occurring in the polymerization of poly(vinyl chloride), the intramolecular 1,5- and 1,6-backbiting and 1,2- and 2,3-Cl shift side reactions. Density functional theory-based reactivity indices combined with an analysis of the reaction force are invoked to probe this concept. The reaction force analysis is used to partition the activation and reaction energy and characterize the behavior of reactivity indices along the three reaction regions that are defined within this approach. It has been observed that in the reactant and product regions mainly geometric rearrangements take place, whereas in the transition state region changes in the electronic bonding pattern occur; here most changes of the electronic properties are observed. The kinetic irreversibility–reversibility of the reactions is confirmed and linked to the differences in the Fukui function and dual descriptor of the radical centers associated with the initial and final species [97].

Allyl monomers are known as poor monomers to yield high molecular weight polymers via polymerization reactions [98]. The abstraction of the reactive allylic hydrogen of the monomer causes chain transfer reactions, which yield decreased molecular weight polymers [99]. Although allyl compounds are not good monomers for polymerization, their difunctional analogs can be polymerized through cyclopolymerization. In a recent work [100], various descriptors, defined within the framework of density functional theory (DFT), are used to explain the regioselectivity of the radical cyclizations preceding the intermolecular propagation step in the cyclopolymerization reactions. The transition states and the activation barriers for both the exo and the endo modes of the cyclization for a number of diallyl radicals are determined. An alternative and recently introduced energy decomposition of the activation barriers is used to investigate the steric effect in the cyclizations. Next, the non-spin-polarized and spin-polarized Fukui functions for a radical attack on the radical conformer minima close to the transition state are computed, in analogy with an earlier study of De Proft et al. [101, 102]. The reactive conformations of the radicals (designated as the reactive rotamers, not the structures corresponding to the global minima) are used for the calculation of the reactivity indices [103]. The regioselectivity in the cyclopolymerization of diallyl monomers is investigated using DFT-based reactivity indices. In the first part, the experimentally observed mode of cyclization (*exo* versus *endo*) of 11

selected radicals involved in this process is reproduced by the computation of activation energies, entropies, enthalpies, and Gibb's free energies for the five- and six-membered cyclization reactions. The application of a recently proposed energy partitioning of the activation barriers shows that the regioselectivity cannot be explained by the steric effect alone. Next, a number of relevant DFT-based reactivity indices, such as nonspin-polarized and spin-polarized Fukui functions, spin densities, and dual descriptors, were applied to probe the role of the polar and stereoelectronic effects in this reaction. The dual descriptor has been found to reproduce best the experimental trends, confirming the important role of the stereoelectronic effects.

The derivative of the Fukui function with respect to the number of electrons is the so-called dual descriptor of chemical reactivity, $f(r)$ [104],

$$f(r) = \left(\frac{\partial f(r)}{\partial N}\right) v = f^{+}(r) - f^{-}(r).$$

Among other things, the dual descriptor is useful for casting the famous Woodward–Hoffmann rules for pericyclic reactions in conceptual DFT [105]. $f(r)$ will be positive in regions of a molecule that are better at accepting electrons than they are at donating electrons, whereas $f(-)(r)$ will be negative in regions that are better at donating electrons than they are at accepting electrons. It is then stated that favorable chemical reactions occur when regions that are good electron acceptors ($f(r) > 0$) are aligned with regions that are good electron donors ($f(r) < 0$) [105].

4.9 Gas Sensor with Single-Wall Carbon Nanotube

In this part, we wish to explore interatomic interaction as well intramolecular interaction through the center of activity. Since the discovery of the structure of carbon nanotubes (CNTs) or single-walled nanotube (SWNT), much effort has been devoted to finding uses of these structures in applications ranging from filed-emission devices to other nano-devices [106, 107]. Kong et al. [108] proposed for the first time the use of CNTs as gas sensors. Experimental data have shown that transport properties of SWNT change dramatically upon exposure to gas molecules at ambient temperature [109]. Main advantage of the open SWNT bundles is that they provide a larger number of adsorption sites. As a result, the adsorption capacity is significantly increased and several new structures and phase transitions were observed [110]. A recent study of Andzelm et al. [111] indicate that the semiconducting SWNTs can serve as gas sensors for several gases like CO, NH_3, H_2, etc. However, NH_3 shows an intriguing behavior compared to other gasses. NH_3 molecule can bind weakly with CNTs, yet can change the conductance significantly. This discrepancy was explained by assuming that the NH_3 binds at defects. For a semiconducting SWNT exposed to 200 ppm of NO_2, it was found that the electrical conductance can increase by three

orders of magnitude in a few seconds. On the other hand, exposure to 2 % NH_3 caused the conductance to decrease up to two orders of magnitude [112]. Sensors made from SWNT have high sensitivity and a fast response time at room temperature, which are important advantages for sensing applications. We have studied the interaction of CNT with different gas molecules such as O_2, N_2, H_2, CO_2, NO_2 to have an understanding of the adsorption behavior of the selected gases in defect-free CNT. We will as well focus on to figure out the effect of variation in the conductance with gas sorption by applying external electric field.

It is very difficult to obtain conductance by quantum mechanical calculation as it will be very much CPU intensive, but measurement of conductance is an utmost important parameter to prove the efficiency of the nanotubes as gas sensors, which is the experimental way of measuring sensors. Thus, a method was developed by calculating the change in the reactivity index before and after the application of the reaction field. The reactivity index provides information about the activity of the gas molecules over SWNT, if the activity changes then the sensing behavior will change [113]. This is a simplistic approach, which is cost-effective to new material design for the sensor industry.

4.10 Excited State Reactivity Index

This study aims to use the concept of ground-state reactivity index formalism within density functional theory (DFT) to predict the behavior of the excited state through the response function produced by weak electric field on chlorinated methanes and chlorinated benzenes. A comparison was made between the geometry of ground state and the excited state for those moieties through configuration interaction (CI) method with Austin Model 1 Hamiltonian over the optimized geometry of DFT at the ground state. Results obtained through these two methodologies suggested that in terms of polarizability and heat of formation, DFT can reproduce the excited state qualitatively. Again, those results can be further validated through UV spectral data, generated using CI method. The reactivity index proposition at ground state shows the potential of DFT to simulate excitation [114].

Primarily, to calculate the reactivity index at the ground state of both the closed systems; methane (CH_4) and benzene (C_6H_6) along with their chlorine-substituted compounds are chosen because methane and benzene is the doorway of the understanding of the properties of larger aliphatic and aromatic compound, respectively. A systematic substitution of hydrogen for both the moieties (methane and benzene) by chlorine was performed to get all the chlorine-substituted products until CCl_4 and C_6Cl_6, respectively. At first, those molecules are optimized with DFT at their neutral state and as well as cationic and anionic forms. The reactivity index values and the relative reactivity indices for individual centers of the series of chlorine-substituted methane and benzene-related compounds were computed. These molecules with the optimized structure were then subjected to the weak electric field to get the response function, followed by CI calculation with

semi-empirical Hamiltonian. The mean polarizability, ionization potential, relative reactive indices, response function and heat of formation as obtained from DFT ground state calculation are compared to the CI excited state. The linear response of the electronic cloud of a chemical species to a weak external electric field is measured in terms of the static electric dipole polarizability. The obtained results were compared with the excited state results from regular CI method.

4.10.1 Absorption Spectra Calculations for Methane (CH_4) Series

All the geometry of CH_4 and chlorine-substituted CH_4 structures are optimized with DFT and then a PECI calculation has been performed. Consequently, the UV spectra of these series of molecules were obtained. The UV spectral data were compared with the experimental results.

4.10.2 Reactivity Index and Polarizability Calculation for Methane (CH_4) Series

The relative reactivity index is calculated, which is the electrophilicity of any site as compared to its own nucleophilicity for the first term and vice versa [74]; for the methane systems with varying amount of Chlorine replacing the hydrogen. The site with highest s_x^+/s_x^- ratio is the most probable site to be attacked by a nucleophile, and electrophilic attack is most feasible when s_x^-/s_x^+ ratio is highest. Those parameters can be used for both intermolecular and intramolecular interactions. To accomplish the change in the ground state activity of CH_4 and its chlorine-substituted compounds, the change of relative nucleophilicity and ionization potential (purely ground state property) was calculated and shown in Fig. 3a. A steady decrease in the relative nucleophilicity with the increasing chlorine substitution in the CH_4 moiety was observed, but there was no significant change in the ionization potential.

Then the polarizability through the response function was calculated using Eqs. (14) and (15) by applying the weak electric filed. The results are shown in Fig. 3b. Interestingly, a similar tendency in terms of polarizability as compared to that of relative nucleophilicity was also found. It has to be mentioned that in response function, a linear response of the electron cloud of a chemical species to the weak external field has been measured in terms of the static electric dipole polarizability, which was quite sensitive to the nature of the bonding, structure of the cluster and eventually related to the ionization potential. To justify the observation of polarizability behavior of a system resulted from the application of weak electric field, it was necessary to observe the polarizability changes in real excited state with multiple excitations.

4.10.3 Reactivity Index and Polarizability Calculation for Benzene (C_6H_6) Series

A steady decrease in the relative nucleophilicity with the increase of chlorine in the benzene moiety has been recognized. However, in contrast to the CH_4 series there

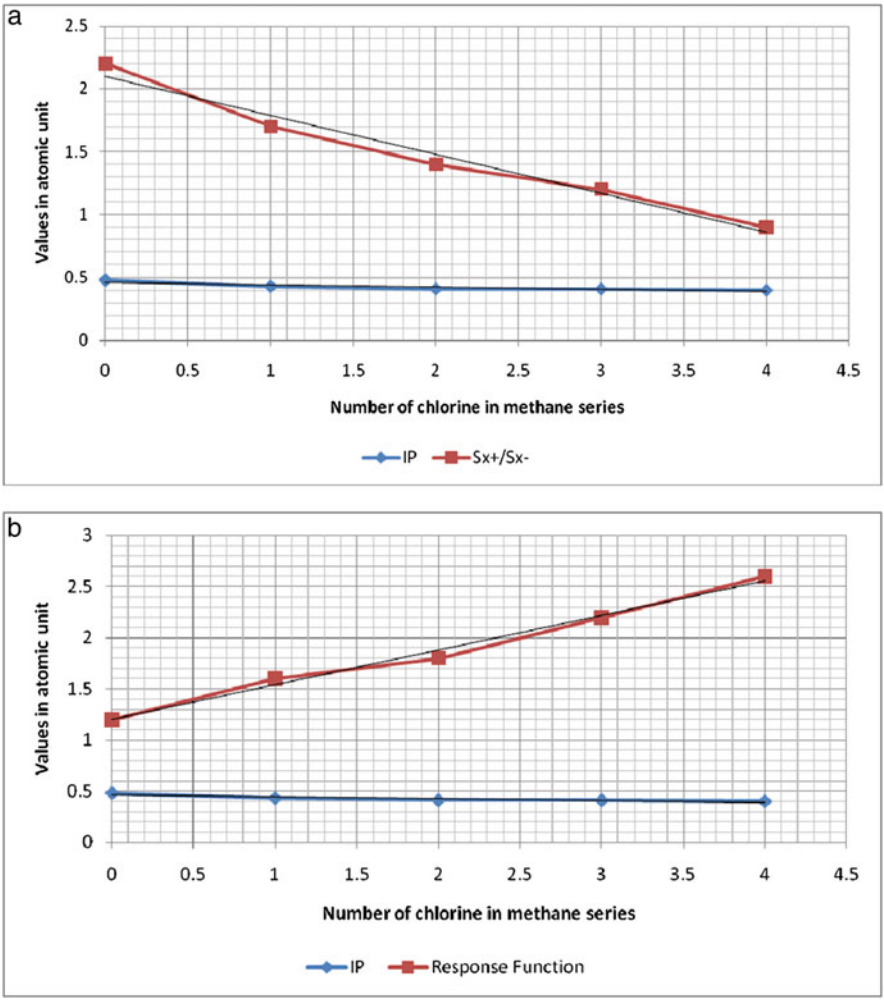

Fig. 3 (**a**) The relative nucleophilicity and ionization potential for the methane series with increase in the chlorine content. (**b**) The change in polarizability and ionization potential for the methane series with increase in the chlorine content, by applying electric field at the ground state

was no significant change in ionization potential with the increasing substitution of the chlorine observed. Moreover, the polarizability in terms of the response function gives a qualitative similarity as that of the relative nucleophilicity.

4.10.4 Comparison of Ground State and Excited State Reactivity Indices for Methane (CH_4) Series

In this communication we have so far performed ground state reactivity index calculation, excited state calculation with CI method whose credibility is validated

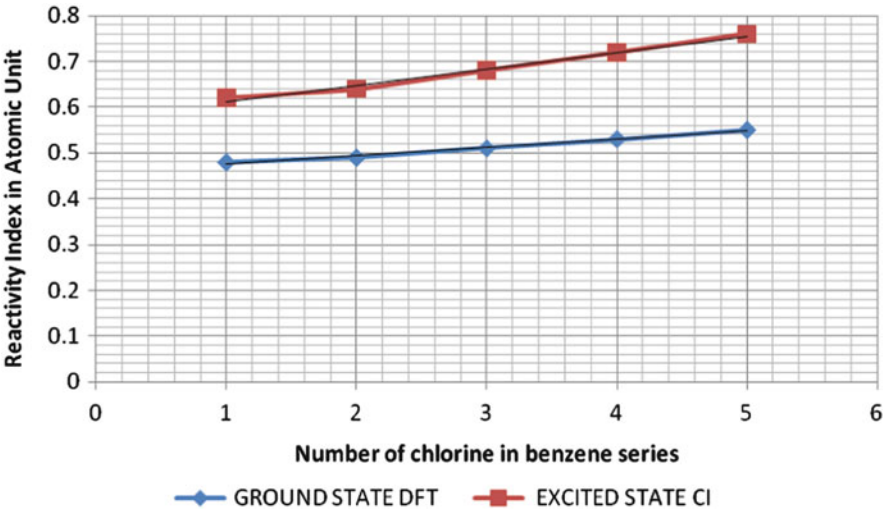

Fig. 4 The relative nucleophilicity as obtained for the benzene series with increase in the chlorine content for both ground state and excited state

with absorption spectral results and as well we have calculated polarizability using the electric field, keeping the goal to see can DFT will be able to reproduce the exited state behavior for the chosen small molecule here methane. To rationalize this, one would expect that reactivity index being a localized parameter should be compared between ground and excited state. The calculated reactivity indices both at the ground state and excited state with two different methodologies are plotted in Fig. 4. The behavioral change with respect to the carbon center present in CH_4 suggested an excellent match between DFT method (ground state) and CI method (excited state), even after the substitution of hydrogen by chlorine.

The test with methane and benzene analogous prove the hypothesis that DFT ground state can produce rationale numbers in excitation which can be comparable with excited state results by CI method. This methodology can now be extrapolated to a reasonable size system specifically for solar cell application with dye sensitized excitations with reasonable accuracy and in a faster calculation time with simple LCAO type DFT methodology.

5 Conclusion

In this review we have revisited the reactivity index theory from HSAB principle within the domain of DFT. We have presented an overview of the reactivity index theory from concept to industrial application. We have demonstrated that a theory within the DFT domain based on the theory of electronegativity and explored in the realm of electron affinity and ionization potential is capable to deliver a simple

correlation to predict the intermolecular and intramolecular interaction. The theory is unique and we are able to describe the origin of the theory and its development down the years. If one can predict the localized interaction between interacting species carefully, then it will be possible to rationalize many chemical phenomena. We here have tried to share with you its capability through the various application examples from the research of our group and as well some recent applications to show that reactivity is an emerging area for material designing from nanocluster through nanowire, nanotube to biomaterial applications. The examples are from all different chemical interactions occurring between different molecular domains. We have shown that the robustness of the theory in terms of its extendibility form localized interaction, to global interactions and as well to a relative scale of implementation. We also have explored the recent development of this theory in excited state. One can therefore use this theory and the indices to rationalize chemical bonding and hence will have the capability to prescribe interactions detrimental for a success of chemical process. We conclude with an optimistic note that the electrophilicity/nucleophilicity will grow from its current tremendous predictive potential, in combination with the related property information for chemical bonding like charge density, orbital overlap integrals, and therefore will be adequate in developing a more expandable theory of chemical interaction removing its limit to reactivity.

References

1. Bronsted JN (1923) Some remarks on the concept of acids and bases, Recueil des Travaux Chimiques des Pays-Bas Volume 42:718–728
2. Lewis GN (1916) The atom and the molecule. J Am Chem Soc 38:762–785
3. Pearson RG (1963) Hard and soft acids and bases. J Am Chem Soc 85:3533–3539
4. Pearson RG (1985) Absolute electronegativity and absolute hardness of Lewis acids and bases. J Am Chem Soc 107:6801–6806
5. Pearson RG (1986) Absolute electronegativity and hardness correlated with molecular orbital Theory. Proc Natl Acad Sci USA 83:8440–8441
6. Pearson RG (1987) Recent advances in the concept of hard and soft acids and bases. J Chem Edu 64:561–567
7. Pearson RG (1988) Absolute electronegativity and hardness: Application to inorganic chemistry. Inorg Chem 27:734–740
8. Pearson RG (1989) Absolute electronegativity and hardness: Application to organic chemistry. Org Chem 54:1423–1430
9. Pearson RG (1997) Chemical Hardness. Wiley-VCH, Weinheim
10. Kohn W, Becke AD, Parr RG (1996) Density functional theory of electronic structure. J Phys Chem 100:12974–12980
11. Putz M.V., (2003) Contributions within Density Functional Theory with Applications in chemical reactivity theory and electronegativity, Dissertation. Com, Parkland, Florida
12. Parr RG, Pearson RG (1983) Absolute hardness: Companion parameter to absolute electronegativity. J Am Chem Soc 105:7512–7516
13. Chattaraj PK, Parr RG (1993) Density functional theory of chemical hardness. Struct Bond 80:11–25
14. Parr RG, Gázquez JL (1993) Hardness functional. J Phys Chem 97:3939–3940

15. Zhou Z, Parr RG (1990) Activation hardness: New index for describing the orientation of electrophilic aromatic substitution. J Am Chem Soc 112:5720–5724
16. Drago RS, Kabler RA (1972) A Quantitative evaluation of the HSAB concept. Inorg Chem 11:3144–3145
17. Chattaraj PK, Lee H, Parr RG (1991) HSAB principle. J Am Chem Soc 113:1855–1856
18. Nalewajski RF (1984) Electrostatic effects in interaction between hard (soft) acids and bases. J Am Chem Soc 106:944–945
19. Chattaraj PK, Sengupta S (1996) Popular electronic structure principles in a dynamical context. J Phys Chem 100:16129–16130
20. Komorowski L, Boyd SL, Boyd RJ (1996) Electronegativity and hardness of disjoint and transferable molecular fragments. J Phys Chem 100:3448–3453
21. Ponti A (2000) DFT-based regioselectivity criteria for cycloaddition reaction. J Phys Chem 104:8843–8846
22. Chandrakumar KRS, Pal S (2002) Study of local hard-soft acid–base principle to multiple-site interactions. J Phys Chem A 106:5737–5744
23. Chandrakumar KRS, Pal S (2002) A systematic study of the reactivity of Lewis acid–base complexes through the local hard-soft acid–base principle. J Phys Chem A 106:11775–11781
24. Chandrakumar KRS, Pal S (2002) Study of local hard-soft acid–base principle: Effects of basis set, electron correlation, and the electron partitioning method. J Phys Chem A 107:5755–5762
25. Chattaraj PK, Maiti B (2003) HSAB principle applied to the time evolution of chemical reactions. J Am Chem Soc 125:2705–2710
26. Putz MV, Russo N, Sicilia E (2004) On the application of the HSAB principle through the use of improved computational schemes for chemical hardness evaluation. J Comput Chem 25:994–1003
27. Torrent-Sucarrat M, Luis JM, Duran M, Solà M (2005) An assessment of a simple hardness kernel approximation for the calculation of the global hardness in a series of Lewis acids and bases. J Mol Struct (THEOCHEM) 727:139–148
28. Kleinert H, Pelster A, Putz MV (2002) Variational perturbation theory for Markov processes. Phys Rev E 65:066128
29. Putz MV, Russo N, Sicilia E (2003) Atomic radii scale and related size properties from density functional electronegativity formulation. J Phys Chem A 107:5461–5465
30. Putz MV (2005) Markovian approach of the electron localization functions. Int J Quantum Chem 105:1–11
31. Putz MV (2006) Systematic formulations for electronegativity and hardness and their atomic scales within density functional softness theory. Int J Quantum Chem 106:361–389
32. Putz MV (2007) Semiclassical electronegativity and chemical hardness. J Theor Comp Chem 6:33–47
33. Putz MV (2008) Maximum hardness index of quantum acid–base bonding. Math Commun Math Comput Chem 60:845–868
34. Putz MV (2009) Electronegativity: quantum observable. Int J Quantum Chem 109:733–738
35. Carey FA, Sundberg RJ (2001) Adv Org Chem; Part B: reactions and synthesis, 4th ed.; Kluwer Academic/Plenum Publishers: New York
36. Lowry TH, Richardson KS (1987) Mechanism and theory in organic chemistry, 3rd edn. Harper & Row, New York
37. Smith MB, March J (2001) Advanced organic chemistry: reactions, mechanisms, and structure, 5th edn. Wiley, New York
38. Sykes P (1970) A guidebook to mechanism in organic chemistry, 6th edn. Orient Longman Limited, New Delhi
39. Parr RG, Szentpaly LV, Liu S (1999) Electrophillicity index. J Am Chem Soc 121:1922–1924

40. Maynard AT, Huang M, Rice WG, Covell DG (1998) Reactivity of the HIV-1 nucleocapsid protein p7 zinc finger domains from the perspective of density-functional theory. Proc Natl Acad Sci U S A 95:11578–11583
41. Fukui K (1973) Theory of orientation and stereoselection. Springer, Berlin
42. Fukui K (1982) Role of frontier orbital in chemical reactions. Science 218:747–754
43. Parr RG, Yang W (1984) Density functional approach to the frontier-electron theory of chemical reactivity. J Am Chem Soc 106:4049–4050
44. Chattaraj PK, Poddar A (1999) Chemical reactivity and excited-state density functional theory. J Phys Chem A 103:1274–1275
45. Geerlings P, De Proft F (2000) HSAB principle: Applications of its global and local forms in organic chemistry. Int J Quantum Chem 80:227–235
46. Ayers PW, Levy M (2000) Perspective on density functional approach to the frontier-electron theory of chemical reactivity. Theor Chem Acc 103:353–360
47. Baeten A, Tafazoli M, Kirsch-Volders M, Geerlings P (1999) Use of the HSAB principle in quantitative structure-activity relationships in toxicological research: Application to the genotoxicity of chlorinated hydrocarbons. Int J Quantum Chem 74:351–355
48. Mendez FDL, Romero M, De Proft F, Geerlings P (1998) The basicity of p-substituted phenolates and the elimination-substitution ratio in p-nitrophenethyl bromide: A HSAB theoretical study. J Org Chem 63:5774–5778
49. Mendez F, Tamariz J, Geerlings P (1998) 1,3-dipolar cycloaddition reactions: A DFT and HSAB principle theoretical model J. Phys Chem A 102:6292–6296
50. Ayers PW, Parr RG, Pearson RG (2006) Elucidating the hard/soft acid/base principle: A perspective based on half-reactions. J Chem Phys 124:194107
51. Ayers PW (2005) An elementary derivation of the hard/soft acid/base principle. J Chem Phys 122:1–3
52. Ayers PW (2007) The physical basis of the global and local hard/soft acid/base principles. Faraday Discuss 135:161–190
53. Parr RG, Chattaraj PK (1991) Principle of maximum hardness. J Am Chem Soc 113:1854–1855
54. Chattaraj PK (1996) Proc Ind Natl Sci Acad Part A 62:513
55. Chattaraj PK, Parr RG (1993) Struct Bonding (Berlin) 80:11
56. Ayers PW, Parr RG (2000) Variational principles for describing chemical reactions: The Fukui function and chemical hardness revisited. J Am Chem Soc 122:2010–2018
57. Torrent-Sucarrat M, Luis JM, Duran M, Sola M (2002) Are the maximum hardness and minimum polarizability principles always obeyed in nontotally symmetric vibrations? J Chem Phys 117:10561–10570
58. Torrent-Sucarrat M, Luis JM, Duran M, Sola M (2001) On the validity of the maximum hardness and minimum polarizability principles for nontotally symmetric vibrations. J Am Chem Soc 123:7951–7952
59. Robles J, Bartolotti LJ (1984) Electronegativities, electron-affinities, ionization potentials and hardness of the elements within spin polarized density functional theory. J Am Chem Soc 106:3723–3727
60. Parr RG, Yang WT (1995) Density functional theory of the electronic-structure of molecules. Ann Rev Phys Chem 46:701–728
61. Geerlings P, De Proft F, Langenaeker W (2003) Conceptual density functional theory. Chem Rev 103:1793–1873
62. Pearson RG (1988) Absolute electronegativity and hardness: application to inorganic chemistry. Inorg Chem 27:734–737
63. Parr RG, Yang WT (1989) Density-functional theory of atoms and molecules. Oxford University Press, New York
64. Vela A, Gazquez JL (1990) A relationship between the static dipole polarizability, the global softness and the Fukui function. J Am Chem Soc 112:1490–1492

65. Chermette H (1999) Chemical reactivity indexes in density functional theory. J Comput Chem 20:129–154
66. Chattaraj PK, Giri S, Duley S (2011) Chem Rev 111:43–75
67. Ayers PW, Anderson JSM, Bartolotti LJ (2005) Perturbative perspectives on the chemical reaction prediction problem. Int J Quantum Chem 101:520–534
68. Chatterjee A, Iwasaki T, Ebina T (1999) Reactivity index scale for interaction of heteroatomic molecules with zeolite framework. J Phys Chem A 103:2489–2494
69. Chatterjee A, Iwasaki T, Ebina T (2001) Best dioctahedral smectite for nitrogen heterocyclics adsorption—A reactivity *index* study. J Phys Chem A 105:10694–10701
70. Chatterjee A, Iwasaki T (2001) A reactivity index study to choose the best template for a particular zeolite synthesis. J Phys Chem A 105:6187–6194
71. Chatterjee A, Iwasaki T, Ebina T, Mizukami F (2003) Intermolecular reactivity studyto scaleadsorptionproperty of para- and meta-substituted dnitrobenzene over 2: 1 dioctahedral smectite. J Chem Phys 118:10212–10220
72. Chatterjee A, Onodera Y, Ebina T, Mizukami F (2003) 2,3,7,8-tetrachloro dibenzo-p-dioxin can be successfully decomposed over 2: 1 dioctahedral smectite—a reactivity index study. J Mol Graph Model 22:93–104
73. Chatterjee A, Suzuki T, Onodera Y, Tanaka DAP (2003) A density functional study to choose the best fluorophore for photon-induced electron-transfer (PET) sensors. Chem Eur J 9:3920–3929
74. Serrano-Andres L, Merchan M (2005) Quantum chemistry of the excited state: 2005 overview. J Mol Struct Theochem 729:99–108
75. Fitzerald G (2008) Molecular simulation, 34, (10–15):931–936
76. Kresse G, Furthmuller J (1996) Efficiency of ab-initio total energy calculations for metals and semiconductors using a plane-wave basis set. Comput Math Sci 6:15–50
77. Rabuck AD, Scuseria GE (1999) Improving self-consistent field convergence by varying occupation numbers. J Chem Phys 110:695–700
78. Roy RK, Krishnamurti S, Geerlings P, Pal S (1998) Local softness and hardness based reactivity descriptors for predicting intra- and intermolecular reactivity sequences: Carbonyl compounds. J Phys Chem A 102:3746–3755
79. Delley B (1990) An all-electron numerical method for solving the local density functional for polyatomic molecules. J Chem Phys 92:508–517
80. Delley B (2000) From molecules to solids with the DMol3 approach. J Chem Phys 113:7756–7764
81. Delley B (1991) Analytical energy derivatives in the numerical local density functional approach. J Chem Phys 94:7245–7250
82. Becke AD (1988) A multicenter numerical-integration scheme for polyatomic molecules. J Chem Phys 88:2547–2553
83. Lee CT, Yang WT, ParrR G (1988) Development of the Colle-Salvetti correlation-energy formula into a functional of the electron density. Phys Rev B 37:785–789
84. Chatterjee A, Onodera Y, Ebina T, Mizukami F (2004) Effect of exchangeable cation on the swelling property of 2: 1 dioctahedral smectite—a periodic first principle study. J Chem Phys 120:3414–3424
85. Berkowitz M, Ghosh SK, Parr RG (1985) On the concept of local hardness in chemistry. J Am Chem Soc 107:6811–6814
86. Yang W, Mortier WJ (1986) The use of global and local molecular parameters for the analysis of the gas-phase basicity of amines. J Am Chem Soc 108:5708–5711
87. Chatterjee A (2002) Edited the special issue on application of density functional theory in chemical reactions. Int J Mol Sci 4:234–444
88. Chatterjee A, Ebina T, Iwasaki T (2003) Adsorption structures and energetic of fluoro- and chlorofluorocarbons over faujasite—a first principle study. Stud Surf Sci Catal 145:371–374

89. Chatterjee A, Ebina T, Iwasaki T, Mizukami F (2003) Cholorofluorocarbons adsorption structures and energetic over faujasite type zeolites—a first principle study. THEOCHEM 630:233–242
90. Chatterjee A, Ebina T, Mizukami F (2005) Effects of water on the structure and bonding of resorcinol in the interlayer of montmorillonite nanocomposite—a periodic first principle study. J Phys Chem B 109:7306–7313
91. Chatterjee A (2006) A reactivity index study to rationalize the effect of dopants on Brönsted and Lewis acidity occurring in MeAlPOs. J Mol Graph Model 24:262–270
92. Saadoune I, Cora F, Catlow CRA (2003) Computational study of the structural and electronic properties of dopant ions in microporous AlPOs. 1. Acid catalytic activity of divalent metal ions. J Phys Chem B 107:3003–3011
93. Chatterjee A, Balaji T, Matsunaga H, Mizukami F (2006) A reactivity index study to monitor the role of solvation on the interaction of the chromophores with amino-functional silanol surface for colorimetric sensors. J Mol Graph Model 25:208–218
94. Chatterjee A, Kawazoe A (2007) Application of the reactivity index to propose intra and intermolecular reactivity in metal cluster interaction over oxide surface. Mater Trans 48:2152–2158
95. Maynard AT, Huang M, Rice WG, Covell DG (1998) Reactivity of the HIV-1 nucleocapsid protein p7 zinc finger domains from the perspective of density-functional theory. Proc Natl Acad Sci USA 95:11578–11583
96. Renato C, Alzate-Morales JH, William T, Santos Juan C, Ca'rdenas C (2007) AQ4 Theoretical study on CDK2 inhibitors using a global softness obtained from the density of states. J Phys Chem B 111:3293–3297
97. Vleeschouwer FD, Toro-Labbe A, Gutie´rrez-Oliva S, Speybroeck V, Waroquier M, Geerlings P, De Proft F (2009) Reversibility from DFT-based reactivity indices: intramolecular side reactions in the polymerization of poly(vinyl chloride). J Phys Chem A 113:7899–7908
98. Zubov VP, Kumar MV, Masterova MN, Kabanov VA (1979) Reactivity of allyl monomers in radical polymerization. J Macromol Sci Chem 1:111–131
99. Matsumoto A (2001) Polymerization of multiallyl monomers. Prog Polym Sci 26:189–257
100. Harada S, Hasegawa S (1984) Homopolymerization of monoallyl ammonium salts with azo initiator. Macromol Chem Rapid Commun 5:27–31
101. Ugur I, Vleeschouwer FD, Tuzun N, Aviyente V, Geerlings P, Liu S, Ayers PW, Proft FD (2009) Cyclopolymerization reactions of diallyl monomers: exploring electronic and steric effects using DFT reactivity indices. J Phys Chem A 113:8704–8711
102. Pinter B, De Proft F, Van Speybroeck V, Hemelsoet K, Waroquier M, Chamorro E, Veszpremi T, Geerlings P (2007) Spin-polarized conceptual density functional theory study of the regioselectivity in ring closures of radicals. J Org Chem 72:348–356
103. Kodaira T, Liu Q-Q, Satoyama M, Urushisaki M, Utsumi H (1999) Cyclopolymerization - XXVI. Repeating unit structure of cyclopolymers derived from N-substituted-N-allyl-2-(methoxycarbonyl)allylamines and mechanism of intramolecular cyclization. Polymer 40:6947–6954, and references therein
104. Morell C, Grand A, Toro-Labbe A (2005) New dual descriptor for chemical reactivity. J Phys Chem A 109:205–212
105. Ayers PW, Morell C, De Proft F, Geerlings P (2007) Understanding the Woodward-Hoffmann rules by using changes in electron density. Chem Eur J 13:8240–8247
106. Ijima S (1991) Helical microtubules of graphitic carbon. Nature 354:56–58
107. De Heer WA, Chatelain A, Ugarte D (1995) A carbon nanotube field-emission electron source. Science 270:1179–1180
108. Kong J, Franklin NR, Zhou CW, Chapline MG, Peng S, Cho KJ, Dai HJ (2000) Nanotube molecular wires as chemical sensors. Science 287:622–625
109. Collins PG, Bradley K, Ishigami M, Zettl A (2000) Extreme oxygen sensitivity of electronic properties of carbon nanotubes. Science 287:1801–1804

110. Jakubek JZ, Simard B (2004) Two confined phases of argon adsorbed inside open single walled carbon nanotubes. Langmuir 20:5940–5945
111. Andzelm J, Govind N, Maiti A (2006) Nanotube-based gas sensors—role of structural defects. Chem Phys Lett 421:58–62
112. Thomas W, Zhou TC, Kong J, Dai H (2000) Gating individual nanotubes and crosses with scanning probes. Appl Phys Lett 76:2412–2416
113. Chatterjee A. Book chapter (2011): Computer simulation to rationalize structure property correlation of Carbon Nano tube. Springer In a book Title: Carbon and oxide nanostructures, edited by Dr. Noorhana Yahya; Advanced Structured Materials 5, 143–164
114. Chatterjee A (2011) Excited state reactivity index theory: application for small moieties. Int J Quantum Chem 111:3821